Localisation of Solar Cell Defects in Luminescence Images using Deep Learning

Zubair Abdullah-Vetter[1], Yoann Buratti[1], Ziv Hameiri[1]

[1]*School of Photovoltaic and Renewable Energy Engineering, University of New South Wales (UNSW), Sydney NSW 2052, Australia*

The growth of the photovoltaic (PV) market is a crucial aspect of addressing climate change using renewable energy [1]. High reliability and durability of PV modules are key requirements for PV to become a main source of energy. Both require fast and accurate detection and classification of defects in solar cells and modules [2]. In this study, we investigate the effectiveness of deep learning algorithms for detection and classification of defects using luminescence images of silicon (Si) solar cells.

Electroluminescence (EL) [3] and photoluminescence (PL) [4] imaging are high-throughput techniques that have been often used for the detection of defects in the PV industry [5], [6]. However, the current visual-based analysis of these images is slow, expensive, requires a relatively deep understanding of solar cell physics and carries inherent bias from the human evaluator [7]. This bias will affect the classification of defects and decisions regarding the required actions. As a result, defect detection can vary between different evaluators [7]. Hence, automated detection using computer vision and machine learning (ML) has recently gained increased attention [7], [8].

Earlier studies in the area of defect detection have used streamlined ML algorithms, where hand crafted feature extraction modules are combined with support vector machine (SVM) or random forest (RF) classifiers [7], [9], [10]. In the past few years, deep learning techniques have been used with increasing success for defect classification [8], [11]. Deep learning has been shown to outperform streamlined algorithms in different fields of research [12], [13]. This has been attributed to increasingly large datasets and a widespread access to stronger computing processors for training the algorithms [14]. The handful of studies that have featured deep learning for defect classification use various imaging techniques including multispectral [15], ultra-violet fluorescence [16] and EL imaging [11], [17]. For EL imaging, it seems that the focus of previous studies has been on field inspection rather than on the manufacturing line [7], [11], [17].

This study aims to incorporate large datasets of luminescence images (PL and EL) of solar cells from manufacturing lines and fielded modules to train deep learning algorithms for automated localisation and classification of faults and defects.

The study is based on over 50,000 unlabelled luminescence images of Si solar cells from partnering companies. It also uses a dataset of over 8,500 labelled images from fielded modules. Both datasets must be labelled to train the deep learning algorithms. Traditionally, images are manually labelled by professionals via visual inspection of the luminescence images [18]. However, due to the very large datasets, such an approach takes a long time. Therefore, this study also aims to develop an unsupervised clustering approach to differentiate and label the remaining images “no-anomaly” cells or “anomaly” cells. The labelled images can then be used to train deep learning models. This initial unsupervised learning approach will require a hand-crafted feature extraction module [19].

To develop the required feature extraction module, the labelled dataset of over 8,500 images is used. A supervised learning pipeline has been developed to test the extracted features by attempting to identify the image labels, which are no-anomaly, cracks, and finger failure. The images are pre-processed through standardising image size, normalising pixel intensity and digitally removing the cells’ busbars. Statistical features, such as the mean and standard deviation of the pixel intensity, are subsequently extracted from these images. An inverted-Otsu [20] thresholding filter is then applied, with the number of remaining pixels being used as another feature. Figure 1 shows the images at each pre-processing stage.

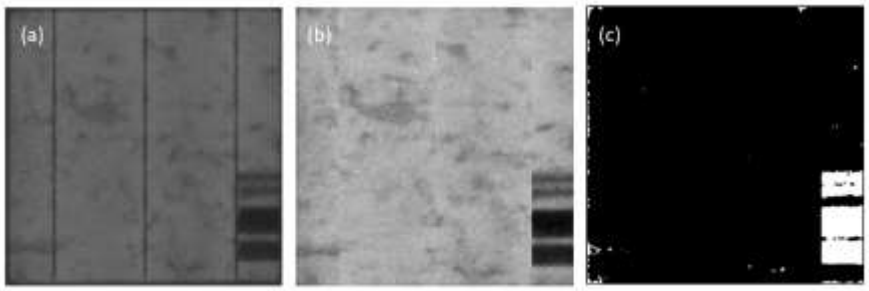

Figure 1 - Example of EL images at the pre-processing stage.
(a) the original image, (b) after pixel intensity normalisation and digital busbar removal, (c) after inverted-Otsu filtering.

To avoid skewing the model (as the number of “no-anomaly” images is much larger than the number of “anomaly” images), the “no-anomaly” images are first down-sampled reducing them to the same number as the “anomaly” cells. The remaining data is then randomly split between training and testing in an 80:20 ratio. The models are then trained on the extracted feature vectors and evaluated with an F1-score [21], the harmonic mean of the precision (positive prediction value) [21] and recall (probability of detection) [21] of the classification results. For hyperparameter tuning, an SVM radial basis function kernel [22] is run five times for each hyperparameter with different randomised down-sampling of “no-anomaly” images and train/test splits, and the resulting F1-score is averaged. The main parameter being tuned is the C-regularisation [23], which controls the margin of classification (a higher C results in a tighter margin). The correct separation of different datapoints is dependent upon the margin of the SVM. The same tuning is repeated another five times to investigate the variance in the training scores due to different randomised down-sampling and train/test splitting.

Figure 2 (a) presents the F1-score as a function of the C-regularisation. Each line represents a different hyperparameter tuning instance. An F1-score of 100% indicates perfect precision and recall [21]. In Figure 2 (b), a confusion matrix is used to visualise the classification results of the SVM model at C-regularisation of 100. The confusion matrix displays the number of predicted and actual classification instances where the diagonal represents the correct predictions for each class. The confusion matrix is also used to calculate the precision, recall, resulting F1-score and accuracy of the classifier model. The preliminary results achieved with this pipeline is an F1-score of 42% and an accuracy of 47%. These results are calculated from the confusion matrix and show that the supervised learning pipeline can still be improved.

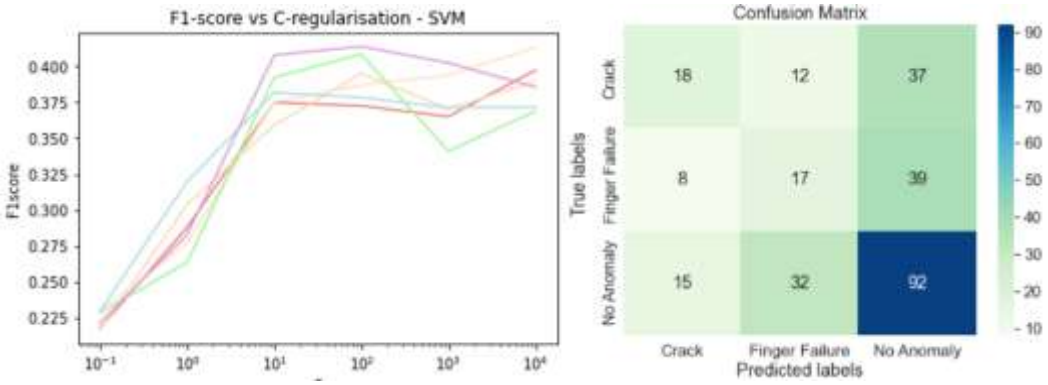

Figure 2 - (a) Hyperparameter tuning results, each line represents a different hyperparameter tuning instance. (b) confusion matrix of the best SVM model.

Future work will include the implementation of different feature extraction and classification algorithms in the supervised learning pipeline. This is followed by automatic labelling of the dataset of over 50,000 EL images with unsupervised clustering. The labelled dataset will subsequently train deep learning models for the localisation and classification of defect sites on the luminescence images of the Si solar cells. For improved defect detection, the labelled dataset will be transferred over existing pre-trained deep learning architectures [24]. The results will be discussed at the conference.

To summarise, automated detection of solar cell defects is an imperative step to maintain the reliability of PV cells and modules. By using very large datasets of luminescence images provided by different partnering companies, this study aims to develop deep learning models capable of localising and classifying defects in Si solar cells. These models will significantly improve the reliability of solar cells and modules by providing fast and accurate automated defect detection in luminescence images of Si solar cells.

References

[1] D. B. Needleman, J. R. Poindexter, R. C. Kurchin, I. M. Peters, G. Wilson, and T. Buonassisi, "Economically sustainable scaling of photovoltaics to meet climate targets," *Energy and Environmental Science*, vol. 9, no. 6, pp. 2122–2129, 2016, doi: 10.1039/C6EE00484A.

[2] M. Demant, T. Welschehold, S. Kluska, and S. Rein, "Microcracks in silicon wafers II: implications on solar cell characteristics, statistics and physical origin," *IEEE Journal of Photovoltaics*, vol. 6, no. 1, pp. 136–144, 2016, doi: 10.1109/JPHOTOV.2015.2465172.

[3] T. Fuyuki, H. Kondo, Y. Kaji, A. Ogane, and Y. Takahashi, "Analytic findings in the electroluminescence characterization of crystalline silicon solar cells," *Journal of Applied Physics*, vol. 101, no. 2, p. 023711, 2007, doi: 10.1063/1.2431075.

[4] T. Trupke, R. A. Bardos, M. C. Schubert, and W. Warta, "Photoluminescence imaging of silicon wafers," *Applied Physics Letters*, vol. 89, no. 4, p. 044107, 2006, doi: 10.1063/1.2234747.

[5] M. Glatthaar, J. Haunschild, M. Kasemann, J. Giesecke, W. Warta, and S. Rein, "Spatially resolved determination of dark saturation current and series resistance of silicon solar cells," *Physica Status Solidi – Rapid Research Letters*, vol. 4, no. 1–2, pp. 13–15, 2010, doi: 10.1002/pssr.200903290.

[6] T. Trupke, E. Pink, R. A. Bardos, and M. D. Abbott, "Spatially resolved series resistance of silicon solar cells obtained from luminescence imaging," *Applied Physics Letters*, vol. 90, no. 9, p. 093506, 2007, doi: 10.1063/1.2709630.

[7] A. M. Karimi *et al.*, "Automated pipeline for photovoltaic module electroluminescence image processing and degradation feature classification," *IEEE Journal of Photovoltaics*, vol. 9, no. 5, pp. 1324–1335, 2019, doi: 10.1109/JPHOTOV.2019.2920732.

[8] S. Deitsch *et al.*, "Automatic classification of defective photovoltaic module cells in electroluminescence images," *Solar Energy*, vol. 185, pp. 455–468, 2019, doi: 10.1016/j.solener.2019.02.067.

[9] S. Anwar and M. Abdullah, "Micro-crack detection of multicrystalline solar cells featuring an improved anisotropic diffusion filter and image segmentation technique," *EURASIP Journal on Image and Video Processing*, vol. 2014, no. 1, pp. 1–17, 2014, doi: 10.1186/1687-5281-2014-15.

[10] B. Su, H. Chen, Y. Zhu, W. Liu, and K. Liu, "Classification of manufacturing defects in multicrystalline solar cells with novel feature descriptor," *IEEE Transactions on Instrumentation and Measurement*, vol. 68, no. 12, pp. 4675–4688, 2019, doi: 10.1109/TIM.2019.2900961.

[11] L. Liu, Y. Zhu, M. R. U. Rahman, P. Zhao, and H. Chen, "Surface defect detection of solar cells based on feature pyramid network and GA-faster-RCNN," in *2nd China Symposium on Cognitive Computing and Hybrid Intelligence*, 2019, pp. 292–297, doi: 10.1109/CCHI.2019.8901952.

[12] K. He, X. Zhang, S. Ren, and J. Sun, "Deep residual learning for image recognition," in *IEEE Conference on Computer Vision and Pattern Recognition*, 2016, pp. 770–778, doi: 10.1109/CVPR.2016.90.

[13] A. Krizhevsky, I. Sutskever, and G. E. Hinton, "ImageNet classification with deep convolutional neural networks," in *Advances in Neural Information Processing Systems*, 2012, pp. 1097–1105.

[14] Y. Lecun, L. Bottou, Y. Bengio, and P. Haffner, "Gradient-based learning applied to document recognition," *Proceedings of the IEEE*, vol. 86, no. 11, pp. 2278–2324, 1998, doi: 10.1109/5.726791.

[15] H. Chen, Y. Pang, Q. Hu, and K. Liu, "Solar cell surface defect inspection based on multispectral convolutional neural network," *Journal of Intelligent Manufacturing*, vol. 31, no. 2, pp. 1–16, 2018, doi: 10.1007/s10845-018-1458-z.

[16] B. Gilleland, W. Hobbs, and J. Richardson, “High throughput detection of cracks and other faults in solar PV modules Using a high-power ultraviolet fluorescence imaging system,” in *46th IEEE Photovoltaic Specialists Conference*, 2019, pp. 2575–2582, doi: 10.1109/PVSC40753.2019.8981262.

[17] A. M. Karimi *et al.*, “Generalized and mechanistic PV module performance prediction from computer vision and machine learning on electroluminescence images,” *IEEE Journal of Photovoltaics*, vol. 10, no. 3, pp. 878–887, 2020, doi: 10.1109/JPHOTOV.2020.2973448.

[18] M. Demant *et al.*, “Microcracks in silicon wafers I: inline detection and implications of crack morphology on wafer strength,” *IEEE Journal of Photovoltaics*, vol. 6, no. 1, pp. 126–135, 2016, doi: 10.1109/JPHOTOV.2015.2494692.

[19] S. Raschka and V. Mirjalili, *Python Machine Learning - third edition*. Birmingham - UK: Packt Publishing, 2019.

[20] N. Otsu, “A threshold selection method from gray-level histograms,” *IEEE Transactions on Systems, Man, and Cybernetics*, vol. 9, no. 1, pp. 62–66, 1979, doi: 10.1109/TSMC.1979.4310076.

[21] S. A. Glantz, *Primer of Applied Regression and Analysis of Variance*. New York - USA: McGraw-Hill Education, 1990.

[22] P. Chudzian, “Radial basis function kernel optimization for pattern classification,” in *Computer Recognition Systems 4*, R. Burduk, M. Kurzyński, M. Woźniak, and A. Żołnierek, Eds. 2011, pp. 99–108.

[23] P. de Boves Harrington, “Support vector machine classification trees,” *Analytical chemistry*, vol. 87, no. 21, pp. 11065–11071, 2015, doi: 10.1021/acs.analchem.5b03113.

[24] W. Zhi, Z. Chen, H. W. F. Yueng, Z. Lu, S. M. Zandavi, and Y. Y. Chung, “Layer removal for transfer learning with deep convolutional neural networks,” vol. 10635, pp. 460–469, 2017, doi: 10.1007/978-3-319-70096-0_48.